

Controlling instability in the Vlasov-Poisson system through moment-based optimization

Jingcheng Lu, Li Wang and Jeff Calder

Abstract

Controlling instability in plasma is one of the central challenges in fusion energy research. Among the various sources of instability, kinetic effects play a significant role. In this work, we aim to suppress the instability induced by kinetic effects by designing an external electric field. However, rather than directly solving the full kinetic Vlasov-Poisson system, we focus on a reduced-order model, specifically the moment-based system, to capture the underlying dynamics. This approach is motivated by the desire to reduce the computational cost associated with repeatedly solving the high-dimensional kinetic equations during the optimization of the electric field. Additionally, moment-based data is more readily accessible in practice, making a moment-based control framework more adaptable to data-driven scenarios. We investigate the effectiveness of moment-based control both analytically and numerically, by comparing it to control based on the full kinetic model.

Contents

1	Introduction	1
2	Suppressing instability with moment systems	4
3	Multiscale analysis of the truncated system	8
3.1	Target error	9
3.2	Model error	10
4	Implementation of moment-based optimization	12
4.1	Derivation of the adjoint state method	13
4.2	Parameter update	15
5	Numerical experiments	15
5.1	Suppressing two-stream instability	15
5.2	Suppressing Bump-on-tail instability	18

1 Introduction

Consider the Vlasov-Poisson (VP) system for the motion of charged particles (e.g. electrons) in plasma state:

$$\left\{ \begin{array}{l} \partial_t f(\mathbf{x}, \mathbf{v}, t) + \mathbf{v} \cdot \nabla_{\mathbf{x}} f(\mathbf{x}, \mathbf{v}, t) + E(\mathbf{x}, t) \cdot \nabla_{\mathbf{v}} f(\mathbf{x}, \mathbf{v}, t) = 0, \\ E(\mathbf{x}, t) = -\nabla_{\mathbf{x}} \phi(\mathbf{x}, t), \\ \nabla_{\mathbf{x}} \cdot E(\mathbf{x}, t) = -\Delta_{\mathbf{x}} \phi(\mathbf{x}, t) = \rho(\mathbf{x}, t) - \rho_{ion}, \\ \rho(\mathbf{x}, t) = \int f(\mathbf{x}, \mathbf{v}, t) d\mathbf{v}. \end{array} \right. \quad (1.1)$$

Here $f(\mathbf{x}, \mathbf{v}, t)$ is particle density at location \mathbf{x} , time t , with velocity \mathbf{v} . We assume that the spatial variable \mathbf{x} lies in a periodic box and the velocity $\mathbf{v} \in \mathbb{R}^d$. This setup is consistent with the modeling of plasma in fusion devices such as in the work of Tokamaks [5]. Here, $E(\mathbf{x}, t)$ is the self-generated electric field, obtained as the negative gradient of a potential function $\phi(\mathbf{x})$, which is determined by the charge density $\rho(\mathbf{x}, t)$ through the Poisson equation in the third line of (1.1). The variable ρ_{ion} is the number density of ions, which neutralize the plasma.

The VP system has been a rich subject of mathematical analysis, with significant work devoted to well-posedness and quantitative properties of solutions [24]. Global well-posedness of classical solutions for large initial data was established in concurrent foundational works by Lions and Perthame [18] and Pfaffelmoser [22], with different techniques. Among the properties of the solutions, one intriguing aspect is the stability (or instability) of the equilibrium upon perturbation. In particular, it is direct to verify that any function depending solely on \mathbf{v} , i.e., $\mu(\mathbf{v})$, constitutes an equilibrium of (1.1), provided the neutrality condition

$$\rho_{ion} = \int_{\mathbb{R}^d} \mu(\mathbf{v}) d\mathbf{v}$$

is satisfied.

When $\mu(\mathbf{v})$ is a Maxwellian distribution, i.e., $\mu(\mathbf{v}) \propto e^{-|\mathbf{v}-u|^2/2T}$ for some given bulk velocity u and temperature T , it is well-known that this equilibrium is stable, in the sense that small perturbations in plasma beams lead to the damping of electrostatic waves, a phenomenon known as Landau damping [17, 19, 20]. In contrast, when $\mu(\mathbf{v})$ is a mixture of two Gaussians, the equilibrium becomes unstable; that is, an initial disturbance in the beams is amplified, leading to undesirable growth of the perturbation and the transfer of energy from the plasma beams to electrostatic waves. If the two Gaussians have comparable magnitudes and are centered opposite about the origin, the resulting instability is referred to as the two-stream instability [4]. Alternatively, if the Gaussians have disparate magnitudes, with the stronger one concentrated near the origin and the weaker one at a larger velocity, the configuration is often termed a bump-on-tail distribution, which is likewise unstable. We also note that (1.1) can admit spatially inhomogeneous equilibrium, which may also be unstable [11]. However, in this work, we focus exclusively on spatially homogeneous equilibria of the form $\mu(\mathbf{v})$.

These instabilities can pose significant challenges in plasma applications. For instance, the two-stream instability, commonly observed in particle accelerators, can lead to unwanted beam scattering and loss of focus [27]. Similarly, in fusion devices, the bump-on-tail instability can arise due to runaway electrons or radiofrequency heating, resulting in a degradation of plasma heating efficiency. It can also cause loss of confinement and the deposition of large amounts of energy onto the reactor walls. Therefore, it is desirable to control these instabilities through carefully designed external forces.

The controllability of VP system was first investigated by Glass and Han-Kwan in [8, 9], where the control is introduced as an external force term. They showed that, for a given initial condition $f_0(\mathbf{x}, \mathbf{v})$, there exists a control that steers the solution to a prescribed final profile $f_1(\mathbf{x}, \mathbf{v})$ at time $t = T$. Later, in a series of papers [14, 15, 16], Knopf and collaborators studied a similar problem: steering the plasma shape at the final time $t = T$ by tuning an external magnetic field. Their main tool was the calculus of variations, through which they analyzed the properties of the control-to-solution map and established necessary and sufficient conditions for the existence of an optimal control. More recently, in [2], they also addressed the problem numerically using a Monte Carlo-based particle-in-cell method. Additionally, Albi et al. [1] recently investigated instantaneous control strategies within the same problem setting.

Another approach aimed at suppressing instability was recently explored in [7], where an external electric field is applied to stabilize the plasma beam and maintain its initial shape. More specifically, replacing E in (1.1) with $E + H$, where H is the external control field, then the goal is to find an optimal

H such that the deviation of f from the equilibrium μ at time $t = T$ is as small as possible:

$$\min_{H \in L^2_{x,t}} \|f(\cdot, \cdot, T; H) - \mu(\cdot)\|_{L^2_{x,v}}. \quad (1.2)$$

In [7], this question is addressed within the PDE-constrained optimization framework. The authors first parameterize H via $H(\mathbf{x}, t; \alpha) = \sum_k \alpha_k \psi_k(\mathbf{x})$, and then determine the coefficients through a hybrid of local and global optimizers. The resulting time independent control is shown to effectively suppress plasma perturbation within the time interval $[0, T]$, but its effectiveness may diminish beyond T . Subsequently, the same problem was revisited using a linear stability analysis approach [6], which leads to the identification of an explicit, time-dependent control based on the precise form of the initial instability.

In this paper, we re-examine the problem (1.2), but instead of using the full VP system (1.1) as the constrained equation, we employ a reduced-order surrogate, namely the hydrodynamic or, more generally, the moment system. This approach is motivated by the concern that optimizing against the full kinetic system (1.1) may be intractable due to the curse of dimensionality. Instead, assessing the validity of the control at the hydrodynamic level offers a more computationally efficient approach. Additionally, in real applications, direct data on the particle distribution is often difficult to obtain, whereas moment-based data is more accessible. Therefore, a moment-based control framework is more easily adaptable to a data-driven scenario.

To facilitate a convenient comparison between kinetic and moment control, we focus on the one-dimensional setting, in which case the VP system (1.1) reduces to

$$\begin{cases} \partial_t f + v \partial_x f + (E + H) \partial_v f = 0, \\ E = -\partial_x \phi, \quad \partial_x E = -\partial_x^2 \phi = \rho - \rho_{ion}, \quad \rho = \int f dv. \end{cases} \quad (1.3)$$

The first three moments of f yield macroscopic quantities defined as:

$$\begin{aligned} \rho(x, t) &:= \int_{\mathbb{R}} f(x, v, t) dv, \\ \rho u(x, t) &:= \int_{\mathbb{R}} v f(x, v, t) dv, \\ \mathcal{E}(x, t) &:= \int_{\mathbb{R}} \frac{v^2}{2} f(x, v, t) dv = \frac{1}{2} p + \frac{1}{2} \rho u^2, \quad \text{where } p(x, t) := \int_{\mathbb{R}} (v - u)^2 f(x, v, t) dv. \end{aligned} \quad (1.4)$$

Integration of (1.3) leads to the Euler-Poisson equations:

$$\begin{cases} \partial_t \rho + \partial_x(\rho u) = 0, \\ \partial_t \rho u + \partial_x(\rho u^2 + p) = \rho(E + H), \\ \partial_t \mathcal{E} + \partial_x((\mathcal{E} + p)u + q) = 0, \\ E = -\partial_x \phi, \quad \partial_x E = -\partial_x^2 \phi = \rho - \rho_{ion}. \end{cases} \quad (1.5)$$

Here, the heat flux $q(x, t) = \int \frac{(v - u)^3}{2} f(x, v, t) dv$ is associated with the third moment of particle distribution f . It can be expressed by ρ , u , \mathcal{E} (or p) by assuming f takes some equilibrium form, in which case (1.5) is then closed.

In general, stability in the fluid regime does not necessarily imply stability when kinetic effects are considered [29, 4]. This is because the VP system (1.1) exhibits much more complex dynamics,

where even spatially homogeneous equilibrium distributions can become unstable, as described above. Therefore, rather than applying control to (1.5), we propose considering a higher-order moment system and investigating its effectiveness as the number of moments increases.

More particularly, we consider the following control problem:

$$\min_H \frac{1}{2} \sum_{n=0}^{\infty} \|m_n(T; H) - \bar{m}_n\|_2^2,$$

$$s.t. \quad \partial_t m_n + \sqrt{n} \partial_x m_{n-1} + \sqrt{n+1} \partial_x m_{n+1} = \sqrt{n} (E + H) m_{n-1}, \quad n = 0, 1, 2, \dots$$

where $m_n(t; H)$ and \bar{m}_n are the moments of the solution $f(t, \cdot, T; H)$ and equilibrium $\mu(\cdot)$, respectively, and their specific definition will be made clear in the next section. E is obtained through m_0 , see (2.7).

In practice, we truncate the moment system at some finite N , and denote the resulting moments as m_n^N , to distinguish them from the full moments m_n . In the next section, we introduce the moment system based on Hermite polynomials and describe a closure rule for the truncated system. Although the truncated moment system provides an approximation to the original Vlasov–Poisson system, and this approximation improves as more moments are included, the impact of truncation on the control outcome is less clear. This issue is explored in section 3, where we compare the optimized electric fields obtained under constraints from the full Vlasov–Poisson system versus those from the truncated moment system. In section 4, we outline the adjoint state method for solving the moment based control problem, and discuss the optimization strategy. Numerical examples are provided in section 5, where we demonstrate the effectiveness of moment based control for two scenarios, two-stream instability and bump-on-tail instability.

2 Suppressing instability with moment systems

In this section, we first lay out our moment systems and then reformulate the control problem as a moment system-constrained optimization. Instead of directly taking the moments of (1.1), as is done previously to lead to (1.5), we derive the moment system using Hermite polynomials in v . This idea dates back to the 90's, where a small finite set of orthogonal polynomials are used to approximate f in v as a numerical method in the Galerkin framework [25, 28, 3].

More specifically, let f be the solution of the Vlasov–Poisson system (1.3) and formally expand it using basis function $\{\mathcal{H}_n(v)\}$:

$$f(x, v, t) = \sum_{n=0}^{\infty} m_n(x, t) \mathcal{H}_n(v), \quad \mathcal{H}_n(v) = \widetilde{\text{He}}_n(v) e^{-\frac{v^2}{2}},$$

where

$$\widetilde{\text{He}}_n(v) = \sqrt{\frac{1}{\sqrt{2\pi n!}}} \text{He}_n(v) \quad \text{with} \quad \text{He}_n(v) = (-1)^n e^{\frac{v^2}{2}} \frac{d^n}{dv^n} e^{-\frac{v^2}{2}}$$

is the normalized Hermite polynomial and satisfies ¹

$$\int_{\mathbb{R}} \widetilde{\text{He}}_m(v) \widetilde{\text{He}}_n(v) w(v) dv = \delta_{mn}, \quad w(v) = e^{-\frac{v^2}{2}}.$$

Here m_n is termed n -th moment and can be defined by

$$m_n(x, t) = \int_{\mathbb{R}} f(x, v, t) \widetilde{\text{He}}_n(v) dv = \sqrt{\frac{1}{\sqrt{2\pi}n!}} \int_{\mathbb{R}} f(x, v, t) \text{He}_n(v) dv.$$

We recall the first few Hermite polynomials:

$$\begin{aligned} \text{He}_0(v) &= 1, \quad \text{He}_1(v) = v, \quad \text{He}_2(v) = v^2 - 1, \\ \text{He}_3(v) &= v^3 - 3v, \quad \text{He}_4(v) = v^4 - 6v^2 + 3, \quad \dots \end{aligned}$$

Following the definition in (1.4), we have

$$\begin{aligned} m_0 &= \sqrt{\frac{1}{\sqrt{2\pi}}} \int_{\mathbb{R}} f dv = \sqrt{\frac{1}{\sqrt{2\pi}}} \rho, \\ m_1 &= \sqrt{\frac{1}{\sqrt{2\pi}}} \int_{\mathbb{R}} v f dv = \sqrt{\frac{1}{\sqrt{2\pi}}} \rho u, \\ m_2 &= \sqrt{\frac{1}{2\sqrt{2\pi}}} \int_{\mathbb{R}} (v^2 - 1) f dv = \sqrt{\frac{1}{2\sqrt{2\pi}}} (2\mathcal{E} - \rho) = \sqrt{\frac{1}{2\sqrt{2\pi}}} (p + \rho u^2 - \rho), \\ m_3 &= \sqrt{\frac{1}{6\sqrt{2\pi}}} \int_{\mathbb{R}} (v^3 - 3v) f dv = \sqrt{\frac{1}{6\sqrt{2\pi}}} (2q + 3pu + \rho u^3 - 3\rho u), \\ &\vdots \end{aligned}$$

The evolution of the moments can be derived from the recursion relations of Hermite polynomials. In particular, we have

$$\begin{aligned} \text{He}_{n+1}(v) &= v \text{He}_n(v) - \text{He}'_n(v), \\ \text{He}_{n+1}(v) &= v \text{He}_n(v) - n \text{He}_{n-1}(v). \end{aligned}$$

Hence the normalized polynomials $\widetilde{\text{He}}_n$ satisfy:

$$\begin{aligned} \sqrt{n+1} \widetilde{\text{He}}_{n+1}(v) &= v \widetilde{\text{He}}_n(v) - \widetilde{\text{He}}'_n(v), \\ \sqrt{n+1} \widetilde{\text{He}}_{n+1}(v) &= v \widetilde{\text{He}}_n(v) - \sqrt{n} \widetilde{\text{He}}_{n-1}(v). \end{aligned} \tag{2.1}$$

¹For unfamiliar readers, we point out that the choice of orthogonal polynomials needs to facilitate two aspects: 1. the appropriate domain of v , e.g., $v \in (-\infty, \infty)$, for Boltzmann equation and Vlasov-Poisson equation, and $v \in [-1, 1]$ for one-dimensional radiative transfer equation; 2. the recursion relation of the orthogonal polynomials needs to fit the structure of the kinetic equation such that after substituting the expansion into the equation, we can get a moment system with simple structure. Taking these aspects into consideration, Hermite polynomials (orthogonal on $v \in (-\infty, \infty)$) and Legendre polynomials (orthogonal on $v \in [-1, 1]$) have been the conventional choice in the derivation of moment systems of high order.

Consequently, we have

$$\begin{aligned}
\partial_t f &= \sum_{n=0}^{\infty} \partial_t m_n \mathcal{H}_n(v), \\
v \partial_x f &= \sum_{n=0}^{\infty} \partial_x m_n v \mathcal{H}_n(v) \\
&= \sum_{n=0}^{\infty} \partial_x m_n (\sqrt{n+1} \mathcal{H}_{n+1}(v) + \sqrt{n} \mathcal{H}_{n-1}(v)) \\
&= \sum_{n=1}^{\infty} \sqrt{n} \partial_x m_{n-1} \mathcal{H}_n(v) + \sum_{n=0}^{\infty} \sqrt{n+1} \partial_x m_{n+1} \mathcal{H}_n(v), \\
(E+H) \partial_v f &= (E+H) \sum_{n=0}^{\infty} m_n (\widetilde{\mathbf{H}} \mathbf{e}_n'(v) - v \widetilde{\mathbf{H}} \mathbf{e}_n(v)) e^{-\frac{v^2}{2}} \\
&= -(E+H) \sum_{n=0}^{\infty} \sqrt{n+1} m_n \widetilde{\mathbf{H}} \mathbf{e}_{n+1}(v) e^{-\frac{v^2}{2}} \\
&= -(E+H) \sum_{n=1}^{\infty} \sqrt{n} m_{n-1} \mathcal{H}_n(v).
\end{aligned}$$

Substituting the above expression into (1.3) yields the corresponding moment equations ²:

$$\begin{aligned}
\partial_t m_0 + \partial_x m_1 &= 0, \\
\partial_t m_1 + \partial_x m_0 + \sqrt{2} \partial_x m_2 &= (E+H) m_0, \\
\partial_t m_2 + \sqrt{2} \partial_x m_1 + \sqrt{3} \partial_x m_3 &= \sqrt{2} (E+H) m_1, \\
&\vdots \\
\partial_t m_N + \sqrt{N} \partial_x m_{N-1} + \sqrt{N+1} \partial_x m_{N+1} &= \sqrt{N} (E+H) m_{N-1}.
\end{aligned} \tag{2.2}$$

Let $\mathbf{m}_N = (m_0, m_1, \dots, m_N)^\top$ consists of moments up to the N -th order, (2.2) can be written into a more compressed form:

$$\frac{\partial \mathbf{m}_N}{\partial t} + A_N \frac{\partial \mathbf{m}_N}{\partial x} = -\sqrt{N+1} \frac{\partial m_{N+1}}{\partial x} \mathbf{e}_{N+1} + (E+H) D_N \mathbf{m}_N, \tag{2.3}$$

where $\mathbf{e}_{N+1} = (0, 0, \dots, 0, 1)^\top$ is the unit vector along the $(N+1)$ -th dimension, and the coefficient matrices are

$$A_N = \begin{bmatrix} 0 & 1 & 0 & 0 & \cdots & 0 & 0 \\ 1 & 0 & \sqrt{2} & 0 & \cdots & 0 & 0 \\ 0 & \sqrt{2} & 0 & \sqrt{3} & \cdots & 0 & 0 \\ \vdots & \vdots & \ddots & \ddots & \ddots & & \vdots \\ \vdots & \vdots & & \ddots & \ddots & \ddots & \vdots \\ 0 & 0 & 0 & \cdots & \sqrt{N-1} & 0 & \sqrt{N} \\ 0 & 0 & 0 & \cdots & 0 & \sqrt{N} & 0 \end{bmatrix}, \tag{2.4}$$

²Note that the definition of moments here is different from (1.4). While (1.4) has a clearer physical interpretation for lower-order moments and is often used in Euler/Navier-Stokes equations, it leads to a highly complicated convection term and thus is inconvenient when deriving equations for higher-order moments. The definition through orthogonal polynomials, due to their recursion relations, will lead to a simpler structure of moment system and is a more common choice for deriving higher-order moment equations. In fact, the two sets of moments can be converted into each other.

and

$$D_N = \begin{bmatrix} 0 & 0 & 0 & 0 & \cdots & 0 & 0 \\ 1 & 0 & 0 & 0 & \cdots & 0 & 0 \\ 0 & \sqrt{2} & 0 & 0 & \cdots & 0 & 0 \\ 0 & 0 & \sqrt{3} & 0 & \cdots & 0 & 0 \\ \vdots & \vdots & \vdots & \ddots & \ddots & \vdots & \vdots \\ \vdots & \vdots & \vdots & & \ddots & 0 & 0 \\ 0 & 0 & 0 & \cdots & \cdots & \sqrt{N} & 0 \end{bmatrix}. \quad (2.5)$$

Due to the symmetry of A_N , the hyperbolicity of the system is guaranteed, and all eigenvalues will be non-zero when N is odd³.

If we also expand the equilibrium state $\mu(x, v) = \sum_{n=0}^{\infty} \bar{m}_n(x) \mathcal{H}_n(v)$, we can then bound the L^2 perturbation of f against μ with moments, that is,

$$\begin{aligned} \int \int |f(x, v, t) - \mu(x, v)|^2 dv dx &= \int \int \left| \sum_{n=0}^{\infty} (m_n(x, t) - \bar{m}_n(x)) \mathcal{H}_n(v) \right|^2 dv dx \\ &= \int \int \left| \sum_{n=0}^{\infty} (m_n(x, t) - \bar{m}_n(x)) \widetilde{\mathcal{H}}_n(v) \right|^2 e^{-v^2} dv dx \\ &\leq \int \int \left| \sum_{n=0}^{\infty} (m_n(x, t) - \bar{m}_n(x)) \widetilde{\mathcal{H}}_n(v) \right|^2 e^{-\frac{v^2}{2}} dv dx \\ &= \sum_{n=0}^{\infty} \int \int (m_n(x, t) - \bar{m}_n(x))^2 \widetilde{\mathcal{H}}_n^2(v) e^{-\frac{v^2}{2}} dv dx \\ &= \sum_{n=0}^{\infty} \|m_n(\cdot, t) - \bar{m}_n(\cdot)\|_2^2. \end{aligned} \quad (2.6)$$

The fourth line is obtained due to the orthogonality of $\{\widetilde{\mathcal{H}}_n(v)\}$ with respect to the weight function $e^{-\frac{v^2}{2}}$. This estimate indicates that if the perturbations of moments are sufficiently suppressed, then the perturbation of the underlying particle distribution will also be suppressed.

Based on the above derivations, we summarize our control problem as follows:

$$\begin{aligned} \min_{\alpha} \quad & \frac{1}{2} \sum_{n=0}^{\infty} \|m_n(T; H) - \bar{m}_n\|_2^2, \\ \text{s.t.} \quad & \partial_t m_k + \sqrt{k} \partial_x m_{k-1} + \sqrt{k+1} \partial_x m_{k+1} = \sqrt{k} (E + H) m_{k-1}, \quad k = 0, 1, 2, \dots; \\ & E = -\partial_x \phi, \quad \partial_x E = -\partial_x^2 \phi = \rho - \rho_{ion}, \quad \rho = (2\pi)^{1/4} m_0; \\ & H(x, t; \alpha) = \sum_k \alpha_k \psi_k(x, t). \end{aligned} \quad (2.7)$$

Here $\psi_k(x, t)$ is a user specified basis that may depend on the prior knowledge of the available control in real experimental set up.

³When N is even, A_N will have eigenvalue 0. Indeed, if we denote $A_{k:N}$ to be the tri-diagonal matrix zero diagonal values, and off diagonal elements being \sqrt{k} to \sqrt{N} . Then one can show that $\det(A_{k:N}) = k \det(A_{k+2:N})$. By induction, it boils down to either a 2×2 matrix $\begin{bmatrix} 0 & \sqrt{N} \\ \sqrt{N} & 0 \end{bmatrix}$ when N is odd or $[0]$ when N is even.

As a comparison, we also recall the original VP constrained control in [7] as follows (see also (1.2)):

$$\begin{aligned} \min_{\alpha} \quad & \frac{1}{2} \|f(T; H) - \mu\|_{L^2_{x,v}}^2, \\ \text{s.t.} \quad & \begin{cases} \partial_t f + v \partial_x f + (E + H) \partial_v f = 0 \\ E = -\partial_x \phi, \quad -\partial_x^2 \phi = \rho - \rho_{ion}, \quad \rho(x, t) = \int f(x, v, t) dv, \\ H(x, t; \alpha) = \sum_k \alpha_k \psi_k(x, t). \end{cases} \end{aligned} \quad (2.8)$$

As written, directly solving the problem (2.7) faces two main challenges:

1. The objective function is expressed as an *infinite* sum of moment perturbations, which is not accessible in practical computations.
2. The original Vlasov-Poisson dynamics corresponds to an *infinite* set of moment equations. However, in practical applications, the moment system is truncated at a finite order, leading to the closure problem for the highest moment.

To address the first issue, a straightforward approach is to truncate the infinite moment perturbations at order N . Naturally, including more moments in the cost function ensures that the perturbation of the particle distribution is more effectively controlled by the moment perturbations. The moment closure problem, however, is more challenging to resolve, as an analytical closure is often unavailable in complex applications, and data-driven approaches are sometimes required [12]. In the context of perturbation suppression, however, a reasonable choice for closure is to use the target equilibrium, that is,

$$\partial_x m_{N+1} \approx \partial_x \bar{m}_{N+1},$$

with $\bar{m}_{N+1}(x) = \int \mu(x, v) \widetilde{\text{He}}_{N+1}(v) dv$. This makes sense because, when the initial perturbation is not too large and with the assistance of an appropriately introduced external field, we expect the solution to remain close to the equilibrium, making $\partial_x \bar{m}_{N+1}$ a good approximation.

Consequently, we further approximate (2.7) to arrive at our final moment-based control problem:

$$\min_{\alpha} \quad \frac{1}{2} \sum_{n=0}^N \|m_n^N(T; \alpha) - \bar{m}_n\|_2^2, \quad (2.9a)$$

subject to the truncated moment system:

$$\begin{cases} \partial_t \mathbf{m}_N^N + A_N \partial_x \mathbf{m}_N^N + \sqrt{N+1} \partial_x \bar{m}_{N+1} \mathbf{e}_{N+1} = (E_N + H) D_N \mathbf{m}_N^N, \\ E_N = -\partial_x \phi_N, \quad -\partial_x^2 \phi_N = \rho_N - \rho_{ion}, \quad \rho_N(x, t) = (2\pi)^{\frac{1}{4}} m_0^N(x, t), \\ H(x, t; \alpha) = \sum_k \alpha_k \psi_k(x, t). \end{cases} \quad (2.9b)$$

Here $\mathbf{m}_N^N = (m_0^N, m_1^N, \dots, m_N^N)$ is the vector of approximate moments. In particular, when a spatially homogeneous equilibrium is considered, we have $\partial_x \bar{m}_{N+1} = 0$.

3 Multiscale analysis of the truncated system

This section is devoted to investigating the connections between the kinetic-based control (2.8) and moment-based control (2.9), particularly the relationship between their respective optimizers H_{VP} and H_{mom} .

In general, the difference between H_{VP} and H_{mom} originates from two main sources:

1. **Target error:** the discrepancy between the distribution perturbation $\frac{1}{2}\|f - \mu\|_{L_{x,v}^2}^2$ and the moment perturbations up to order $\frac{1}{2}\sum_{n=0}^N \|m_n^N - \bar{m}_n\|_{L_x^2}^2$;
2. **Model error:** the deviation between the exact Vlasov–Poisson system and the truncated moment system (2.9b).

3.1 Target error

The target error arises from the truncation of the infinite series $\sum_{n=0}^{\infty} \|m_n - \bar{m}_n\|_{L_x^2}^2 = \|f - \mu\|_{w_v^{-1}L_x^2}^2$ to a finite sum. This error generally depends on the regularity of the function. Since the truncation occurs only in the v -variable, we first present the following proposition for functions depending solely on v . The extension to functions depending on both x and v is straightforward.

Proposition 3.1. *Consider a function $g(v)$ such that $\|g\|_{w_v^{-1}} < +\infty$. Expand g as*

$$g = \sum_{l=0}^{\infty} \hat{g}_l \widetilde{\text{He}}_l(v) e^{-\frac{v^2}{2}}, \quad \text{where } \hat{g}_l = \int_{\mathbb{R}} g(v) \widetilde{\text{He}}_l(v) dv. \quad (3.1)$$

Then define an operator $\mathcal{A}g := \partial_v g + vg$, we have:

$$\sum_{l=N+1}^{\infty} |\hat{g}_l|^2 \lesssim N^{-k} \|\mathcal{A}^k g\|_{w_v^{-1}}^2. \quad (3.2)$$

This proposition can be viewed as a variation of [26, Theorem 7.13] or [10, Lemma 2.5], with the main difference being how we define the moments (or spectral coefficients). We also note that the bound we derive imposes a rather strong condition on g . Specifically, g must not only be sufficiently regular, as required by the repeated application of the operator \mathcal{A} , but it also needs to exhibit sufficient decay at the tail. This is because the k -th weighted moments of g , weighted by the rapidly growing function $e^{\frac{v^2}{2}}$ must be bounded. One example of such a function g that satisfies this condition is a Gaussian distribution.

Proof. Note first that $\widetilde{\text{He}}$ satisfies the following relation $\frac{d}{dv}(e^{-\frac{v^2}{2}} \frac{d}{dv} \widetilde{\text{He}}_n) = -\lambda_n e^{-\frac{v^2}{2}} \widetilde{\text{He}}_n$ with $\lambda_n = n$, we have

$$\begin{aligned} \int_{\mathbb{R}} g(v) \widetilde{\text{He}}_n(v) dv &= -\frac{1}{\lambda_n} \int_{\mathbb{R}} g(v) e^{\frac{v^2}{2}} \frac{d}{dv} (e^{-\frac{v^2}{2}} \frac{d}{dv} \widetilde{\text{He}}_n) dv \\ &= \frac{1}{\lambda_n} \int_{\mathbb{R}} \frac{d}{dv} (g(v) e^{\frac{v^2}{2}}) (e^{-\frac{v^2}{2}} \frac{d}{dv} \widetilde{\text{He}}_n) dv \\ &= \frac{1}{\lambda_n} \int_{\mathbb{R}} \mathcal{A}g \frac{\sqrt{c_{n-1}}}{\sqrt{c_n}} \lambda_n \widetilde{\text{He}}_{n-1} dv, \quad c_n := n! \sqrt{2\pi} \end{aligned}$$

where the last equality uses the fact $\sqrt{c_n} \widetilde{\text{He}}'_n(v) = \lambda_n \sqrt{c_{n-1}} \widetilde{\text{He}}_{n-1}(v)$. Repeat the above process we get

$$g_n = \int_{\mathbb{R}} g(v) \widetilde{\text{He}}_n(v) dv = \frac{\sqrt{c_{n-k}}}{\sqrt{c_n}} \int_{\mathbb{R}} \mathcal{A}^k g \widetilde{\text{He}}_{n-k} dv. \quad (3.3)$$

Consequently,

$$\begin{aligned} \sum_{l=N+1}^{\infty} |\hat{g}_l|^2 &= \sum_{l=N+1}^{\infty} \frac{c_{l-k}}{c_l} \left(\int_{\mathbb{R}} \mathcal{A}^k g \widetilde{\text{He}}_{l-k} dv \right)^2 \\ &\leq \max_{l \geq N+1, l \geq k} \frac{c_{l-k}}{c_l} \sum_{l=N+1}^{\infty} \left(\int_{\mathbb{R}} \mathcal{A}^k g \widetilde{\text{He}}_{l-k} dv \right)^2 \lesssim N^{-k} \|\mathcal{A}^k g\|_{w_v^{-1}}^2. \end{aligned}$$

The last inequality is obtained by noticing that $\|g\|_{w_v^{-1}}^2 = \sum_{n=0}^{\infty} |\hat{g}_n|^2 = \sum_{n=0}^{\infty} \left(\int_{\mathbb{R}} g(v) \widetilde{\text{He}}_n(v) dv \right)^2$. \square

As an immediate consequence of Proposition 3.1, we have

Corollary 3.2. *Let $m_n(x, t) = \int_{\mathbb{R}} f(x, v, t) \widetilde{\text{He}}_n(v) dv$ and $\bar{m}_n = \int_{\mathbb{R}} \mu(v) \widetilde{\text{He}}_n(v) dv$, then*

$$\sum_{n=N+1}^{\infty} \|m_n - \bar{m}_n\|_{L_x^2}^2 \lesssim N^{-k} \|\mathcal{A}^k(f - \mu)\|_{w_v^{-1} L_x^2}^2.$$

3.2 Model error

To quantify the model error, we propose the following auxiliary function f_N , which maps the moment information to an approximate distribution function:

$$f_N(x, v, t) = \mu(v) + \sum_{n=0}^N (m_n^N(x, t) - \bar{m}_n) \mathcal{H}_n(v). \quad (3.4)$$

Clearly, following the lines of (2.6), we have

$$\frac{1}{2} \|f_N - \mu\|_{L_{x,v}^2}^2 = \frac{1}{2} \left\| \sum_{n=0}^N (m_n^N - \bar{m}_n) \mathcal{H}_n \right\|_{L_{x,v}^2}^2 \leq \frac{1}{2} \sum_{n=0}^N \|m_n^N - \bar{m}_n\|_2^2. \quad (3.5)$$

Notably, the upper bound on the right-hand side corresponds exactly to the objective function (2.9a) in the moment-based optimization. This implies that the optimized external field, H_{mom} , constrained by the truncated moment system, effectively suppresses the perturbation of the approximate distribution f_N from the equilibrium μ .

To characterize the evolution of f_N under ansatz (3.4), we use the recursion (2.1) and derive

$$\begin{aligned} \partial_t f_N + v \partial_x f_N + (E_N + H) \partial_v f_N &= \sum_{n=0}^N [\partial_t m_n^N + \sqrt{n} \partial_x m_{n-1}^N + \sqrt{n+1} \partial_x m_{n+1}^N - (E_N + H) \sqrt{n} m_{n-1}^N] \mathcal{H}_n \\ &\quad + \sqrt{N+1} \partial_x m_N^N \mathcal{H}_{N+1} - (E_N + H) \sqrt{N+1} m_N^N \mathcal{H}_{N+1} \\ &\quad + (E_N + H) \partial_v \left(\mu - \sum_{n=0}^N \bar{m}_n \mathcal{H}_n \right) \\ &= \sqrt{N+1} \partial_x m_N^N \mathcal{H}_{N+1} - (E_N + H) \sqrt{N+1} m_N^N \mathcal{H}_{N+1} \\ &\quad + (E_N + H) \partial_v \left(\mu - \sum_{n=0}^N \bar{m}_n \mathcal{H}_n \right) \end{aligned}$$

Using the relation $\sqrt{n+1}\mathcal{H}_{n+1}(v) = -\mathcal{H}'_n(v)$, the above equation can be simplified to:

$$\begin{cases} \partial_t f_N + v\partial_x f_N + (E_N + H)\partial_v \left(\sum_{n=0}^{N-1} m_n^N \mathcal{H}_n \right) = \sqrt{N+1} \partial_x m_N^N \mathcal{H}_{N+1}, \\ E_N = -\partial_x \phi_N, \quad -\partial_x^2 \phi_N = \rho_N - \rho_{ion} \\ \rho_N = \int f_N dv. \end{cases} \quad (3.6)$$

In this way, the dynamics described by (3.6) provide an equivalent kinetic representation of the moment system (2.9b), enabling a direct comparison with the exact Vlasov–Poisson system.

More specifically, we compare the two control problems:

- 1) Our moment control: $\min_{H_{mom}} \|f_N - \mu\|^2$ subject to (3.6);
- 2) Original control: $\min_{H_{VP}} \|f - \mu\|^2$ subject to (1.3).

For this purpose, we adopt a linearized approach, following the methodology used in the derivation of the Penrose condition [21], the proposal of Landau damping by Landau [17], and, more recently, the work of Einkemmer et al. [6] in designing controlled electric fields.

Let f and f_N be the particle distributions in the true physics (1.3) and the moment based system (3.6), respectively. We assume f and f_N are small perturbations around the equilibrium μ as:

$$\delta f := f - \mu \ll \mu, \quad \delta f_N := f_N - \mu \ll \mu, \quad m_n^N - \bar{m}_n \ll \bar{m}_n.$$

Then (1.3) and (3.6) can be linearized into

$$\partial_t \delta f + v\partial_x \delta f + (E + H)\partial_v \mu = 0, \quad (3.7)$$

and

$$\partial_t \delta f_N + v\partial_x \delta f_N + (E_N + H)\partial_v \mu_{N-1} = \sqrt{N+1} \partial_x m_N^N \mathcal{H}_{N+1}, \quad \mu_{N-1}(v) = \sum_{n=0}^{N-1} \bar{m}_n \mathcal{H}_n(v). \quad (3.8)$$

Likewise, we define the perturbation densities,

$$\delta \rho(x, t) = \int \delta f(x, v, t) dv, \quad \delta \rho_N(x, t) = \int \delta f_N(x, v, t) dv,$$

and, for convenience of discussion, assume that

$$\delta f(x, v, 0) = \delta f_N(x, v, 0) = \delta f_0(x, v).$$

By performing Fourier and Laplace transforms on equation (3.7), it was shown in [6, Appendix B] that the density perturbation can be described with

$$\mathcal{L}[\widehat{\delta \rho}(\xi, \cdot)](s) = \mathcal{L}[\widehat{\delta \rho_F}(\xi, \cdot)](s) - \frac{i\xi \mathcal{L}[\widehat{H}(\xi, \cdot)](s) + \mathcal{L}[\widehat{\delta \rho_F}(\xi, \cdot)](s)}{1 + \mathcal{L}[\widehat{U}(\xi, \cdot)](s)} \mathcal{L}[\widehat{U}(\xi, \cdot)](s), \quad (3.9)$$

where $\widehat{\cdot}$ represents Fourier transform in space, $\mathcal{L}[\cdot]$ represents Laplace transform in time. The function $U(x, t)$ satisfies

$$\widehat{U}(\xi, t) = t\widehat{\mu}(t\xi), \quad (3.10)$$

and

$$\delta\rho_F(x, t) = \int \delta f_F(x, v, t) dv \quad (3.11)$$

is the free stream perturbation density where $\delta f_F(x, v, t) = \delta f_0(x - vt, v)$ satisfies the free stream transport $\partial_t \delta f_F + v \partial_x \delta f_F = 0$. Applying similar derivations to (3.8), we obtain

$$\begin{aligned} \mathcal{L}[\widehat{\delta\rho_N}(\xi, \cdot)](s) &= \mathcal{L}[\widehat{\delta\rho_F}(\xi, \cdot)](s) - \frac{i\xi \mathcal{L}[\widehat{H}(\xi, \cdot)](s) + \mathcal{L}[\widehat{\delta\rho_F}(\xi, \cdot)](s)}{1 + \mathcal{L}[\widehat{U_{N-1}}(\xi, \cdot)](s)} \mathcal{L}[\widehat{U_{N-1}}(\xi, \cdot)](s) \\ &\quad + \frac{i\xi \sqrt{N+1} \mathcal{L}[m_N^N(\xi, \cdot)](s)}{1 + \mathcal{L}[\widehat{U_{N-1}}(\xi, \cdot)](s)} \mathcal{L}[\widehat{\mathcal{H}_{N+1}}(\xi, \cdot)](s), \end{aligned} \quad (3.12)$$

where

$$\widehat{U_{N-1}}(\xi, t) = t \widehat{\mu_{N-1}}(t\xi) = t \sum_{n=0}^{N-1} \overline{m}_n \widehat{\mathcal{H}}_n(t\xi), \quad \widehat{\mathcal{H}}_{N+1}(t\xi) = \int \mathcal{H}_{N+1}(v) e^{-i(\xi t)v} dv.$$

Then, if we consider choosing the external field H to cancel the self-generated electric field, as suggested in [6, Section 3.1], we obtain the following result concerning the difference between the two control problems.

Proposition 3.3. *Let H_{mom} and H_{VP} denote the control fields for systems (3.6) and (1.3) respectively. Suppose these fields are selected to cancel the self-generated electric field, that is,*

$$i\xi \mathcal{L}[\widehat{H_{VP}}] = -\mathcal{L}[\widehat{\delta\rho_F}] \quad (3.13)$$

$$i\xi \mathcal{L}[\widehat{H_{mom}}] = -\mathcal{L}[\widehat{\delta\rho_F}] + \frac{i\xi \sqrt{N+1}}{\mathcal{L}[\widehat{U_{N-1}}]} \mathcal{L}[m_N^N] \mathcal{L}[\widehat{\mathcal{H}_{N+1}}] \quad (3.14)$$

where $\delta\rho_F$ is defined in (3.11), and $\mathcal{L}[\widehat{H}]$ is a short notation for $\mathcal{L}[\widehat{H}(\xi, \cdot)](s)$. Then, if the equilibrium \widehat{U} (corresponding to μ by (3.10)) has the property that $|\mathcal{L}[\widehat{U_{N-1}}]|$ is bounded away from zero independent of N , the difference between the two control fields satisfies

$$|\mathcal{L}[\widehat{H_{mom}}] - \mathcal{L}[\widehat{H_{VP}}]| = \left| \frac{\mathcal{L}[\widehat{\mathcal{H}_{N+1}}]}{\mathcal{L}[\widehat{U_{N-1}}]} \sqrt{N+1} \mathcal{L}[m_N^N] \right| \lesssim \frac{\sqrt{N+1}}{N^{k/2}} \|\mathcal{A}^k f_N\|_{w_v^{-1} L_x^2}, \quad (3.15)$$

where \mathcal{A} is again defined by $\mathcal{A}g := \partial_v g + vg$. Additionally, if we use the \widehat{H}_{mom} obtained from moment control system to control the original Vlasov-Poisson system, we obtain the following perturbation:

$$\mathcal{L}[\widehat{\delta\rho}] = \mathcal{L}[\widehat{\delta\rho_F}] - \frac{\mathcal{L}[\widehat{U}]}{1 + \mathcal{L}[\widehat{U}]} \frac{i\xi \mathcal{L}[\widehat{\mathcal{H}}_N]}{\mathcal{L}[\widehat{U_{N-1}}]} \sqrt{N+1} \mathcal{L}[m_N^N].$$

Proof. The derivation of (3.13) and (3.14) is straightforward from (3.9) and (3.12), respectively. The estimate (3.15) follows from the fact that $|\mathcal{H}_N| \lesssim e^{-\frac{v^2}{4}}$ and the application of Corollary 3.2. \square

4 Implementation of moment-based optimization

This section is devoted to solving the moment-based control problem (2.9), using the classical adjoint state method. The implementation details are outlined as follows.

4.1 Derivation of the adjoint state method

We consider the constraint moment system,

$$\frac{\partial \mathbf{m}}{\partial t} + A \frac{\partial \mathbf{m}}{\partial x} + \sqrt{N+1} \frac{\partial \bar{m}_{N+1}}{\partial x} \mathbf{e}_{N+1} = (E_N + H) D \mathbf{m}, \quad (4.1)$$

where $\mathbf{m} = (m_0^N, m_1^N, \dots, m_N^N)^\top$, $H(x, t; \alpha) = \sum_k \alpha_k \psi_k(x, t)$, and the constant coefficient matrices A , D are given in (2.4) and (2.5). Here we omit the N in the superscripts and subscripts of \mathbf{m}_N^N , A_N , D_N for notation simplicity.

Our goal is to optimize the external field $H(x, t; \alpha)$ such that the L^2 -moment perturbation can be sufficiently suppressed:

$$L(\{\mathbf{m}(T; \alpha)\}) = \frac{1}{2} \|\mathbf{m}(T; \alpha) - \bar{\mathbf{m}}\|_2^2 = \sum_{n=0}^N \frac{1}{2} \int |m_n(x, T; \alpha) - \bar{m}_n|^2 dx,$$

where $\bar{m}_n = \int \mu(v) \widetilde{\text{He}}_n(v) dv$ is the n -th moment of the desired equilibrium μ . We intend to optimize the parameters α using the gradient descent iterations. To this end, we introduce the Lagrangian multiplier $\lambda(x, t)$ and set

$$\mathcal{L}(\{\mathbf{m}(T; \alpha)\}) = L(\{\mathbf{m}(T; \alpha)\}) + \int_0^T \int \lambda(x, t)^\top (\partial_t \mathbf{m} + A \partial_x \mathbf{m} + \sqrt{N+1} \partial_x \bar{m}_{N+1} \mathbf{e}_{N+1} - (E_N + H) D \mathbf{m}) dx dt.$$

Obviously, when $\mathbf{m}(x, t)$ satisfies the equation (4.1) we have $\mathcal{L}(\{\mathbf{m}(T)\}) = L(\{\mathbf{m}(T)\})$ for any arbitrary choice of λ .

Taking the gradient of \mathcal{L} with respect to α_k , we have

$$\begin{aligned} \frac{\partial \mathcal{L}}{\partial \alpha_k} &= \int (\mathbf{m}(x, T) - \bar{\mathbf{m}})^\top \partial_{\alpha_k} \mathbf{m}(x, T) dx + \int_0^T \int \lambda(x, t)^\top (\partial_t \partial_{\alpha_k} \mathbf{m} + A \partial_x \partial_{\alpha_k} \mathbf{m} - (E_N + H) D \partial_{\alpha_k} \mathbf{m}) dx dt \\ &\quad - \int_0^T \int \lambda(x, t)^\top (\partial_{\alpha_k} E_N(x, t) + \psi_k(x, t)) D \mathbf{m}(x, t) dx dt \\ &= \int (\mathbf{m}(x, T) - \bar{\mathbf{m}} + \lambda(x, T))^\top \partial_{\alpha_k} \mathbf{m}(x, T) dx - \int_0^T \int \{\partial_t \lambda^\top + \partial_x \lambda^\top A + \lambda^\top (E_N + H) D\} \partial_{\alpha_k} \mathbf{m} dx dt \\ &\quad - \int_0^T \int \lambda(x, t)^\top (\partial_{\alpha_k} E_N(x, t) + \psi_k(x, t)) D \mathbf{m}(x, t) dx dt, \end{aligned} \quad (4.2)$$

where the second equality uses integration by parts. To avoid the expensive evaluation of $\partial_{\alpha_k} \mathbf{m}$, we let λ solving the following space-time continuous adjoint equations

$$\begin{cases} \partial_t \lambda(x, t) + A^\top \partial_x \lambda(x, t) = -(E_N(x, t) + H(x, t)) D^\top \lambda(x, t), \\ \lambda(x, T) = -(\mathbf{m}(x, T) - \bar{\mathbf{m}}). \end{cases} \quad (4.3)$$

Then the gradient of the loss function reduces to

$$\frac{\partial L}{\partial \alpha_k} = \frac{\partial \mathcal{L}}{\partial \alpha_k} = - \int_0^T \int \lambda(x, t)^\top (\partial_{\alpha_k} E_N(x, t) + \psi_k(x, t)) D \mathbf{m}(x, t) dx dt. \quad (4.4)$$

Note that in the gradient expression (4.4), the term $\partial_{\alpha_k} E_N$ is the most computationally involved. However, to better understand this term, consider its underlying structure. Let $G(x, x')$ be the Green's function to the 1D Poisson equation with appropriate boundary conditions. Then we have

$$\partial_{\alpha_k} E_N(x, t) = - \int \partial_x G(x, x') \partial_{\alpha_k} \delta \rho_N(x', t) dx',$$

where $\delta\rho_N = \rho_N - \bar{\rho}$ is the density perturbation. Hence, under the assumption of small perturbations, we have $|\partial_{\alpha_k} E_N(x, t)| \ll 1$ and can be safely omitted. Consequently, we will only use the following approximate gradient in the optimization:

$$\frac{\partial L}{\partial \alpha_k} \approx - \int_0^T \int \lambda(x, t)^\top \psi_k(x, t) D\mathbf{m}(x, t) dx dt. \quad (4.5)$$

Such simplification turns out to generate satisfactory results for moderate perturbations, as will be shown in section 5. When more accurate gradient calculation is needed, modern scientific computing packages such as `torchdiffeq` can be used for numerical auto-differentiation.⁴

To discretize the moment system (4.1) as well as the the adjoint equations (4.3), we will use the semi-Lagrangian method combined with Strang splitting. Since the matrix A is symmetric, we can diagonalize it in the form

$$A = R\Lambda R^{-1}, \quad R = [\mathbf{r}_0, \mathbf{r}_1, \dots, \mathbf{r}_N], \quad \Lambda = \text{diag}(\lambda_0, \lambda_1, \dots, \lambda_N),$$

where $\lambda_0, \dots, \lambda_N$ are the eigenvalues of A , $\mathbf{r}_0, \dots, \mathbf{r}_N$ are the corresponding eigenvectors. They are obtained numerically with Matlab's `eig` solver. We define the characteristic variables

$$\mathbf{w}(x, t) = R^{-1}\mathbf{m}(x, t).$$

Multiplying (4.1) by R^{-1} on the left yields

$$\frac{\partial}{\partial t} \mathbf{w}(x, t) + \Lambda \frac{\partial}{\partial x} \mathbf{w}(x, t) = \tilde{F}(x, t), \quad \tilde{F}(x, t) = (E(x, t) + H(x, t)) R^{-1} D\mathbf{m}(x, t),$$

or equivalently,

$$\partial_t w_k(x, t) + \lambda_k \partial_x w_k(x, t) = \tilde{F}_k(x, t), \quad k = 0, 1, \dots, N, \quad (4.6)$$

where w_k and \tilde{F}_k are the k -th component of \mathbf{w} and \tilde{F} . Applying semi-Lagrangian to (4.6) (or equivalently (4.1)) with grid points $\{x_j\}$ and time step Δt , we have:

- Compute

$$w_k^{n+\frac{1}{2}}(x_j) = w_k(x_j - \frac{\Delta t}{2} \lambda_k, t^n), \quad k = 0, 1, \dots, N \implies \mathbf{m}^{n+\frac{1}{2}}(x_j) = R\mathbf{w}^{n+\frac{1}{2}}(x_j).$$

- Compute

$$\mathbf{m}^{n+1,*}(x_j) = \mathbf{m}^{n+\frac{1}{2}}(x_j) + \Delta t F^{n+\frac{1}{2}}(x_j),$$

where $F^{n+\frac{1}{2}}(x_j) = (E_N^{n+\frac{1}{2}}(x_j) + H(x_j, t^{n+\frac{1}{2}})) D\mathbf{m}^{n+\frac{1}{2}}(x_j)$, $E_N^{n+\frac{1}{2}}(x_j)$ is computed from the density $\rho_N^{n+\frac{1}{2}} = (2\pi)^{\frac{1}{4}} m_0^{n+\frac{1}{2}}$. We also compute the characteristic variables

$$\mathbf{w}^{n+1,*}(x) = R^{-1}\mathbf{m}^{n+1,*}(x).$$

- Compute

$$w_k^{n+1}(x_j) = w_k^{n+1,*}(x_j - \frac{\Delta t}{2} \lambda_k), \quad k = 0, 1, \dots, N \implies \mathbf{m}^{n+1}(x_j) = R\mathbf{w}^{n+1}(x_j).$$

$\mathbf{m}^{n+1}(x_j)$ is then taken as the approximation to $\mathbf{m}(x_j, t^{n+1})$. In the first and third steps, we use linear interpolation to obtain the nodal values at $x_j - \frac{\Delta t}{2} \lambda_k$. The backward integration of the adjoint PDE (4.3) can be derived in a similar manner.

⁴For more reference, see <https://github.com/rtqichen/torchdiffeq>

4.2 Parameter update

To update the parameters, we employ the gradient descent method with momentum to accelerate the convergence. Starting with zero momentum $w^{(0)} = 0$, we update α with

$$\begin{cases} w^{(i+1)} = \beta w^{(i)} + \nabla_{\alpha} L^{(i)} \\ \alpha^{(i+1)} = \alpha^{(i)} - \eta^{(i+1)} w^{(i+1)} \end{cases}, \quad i = 0, 1, 2, \dots, \quad (4.7)$$

where the weight $\beta \in [0, 1)$ measures the strength of inertia, $\eta^{(i)}$ is the learning rate at the i -th iteration. Such acceleration protocol dates back to Polyak's heavy ball method [23]. A large value of β indicates that the iterations are strongly affected by the previous updates. When $\beta = 0$, it reduces to the vanilla gradient descent.

To determine the appropriate learning rate for each parameter, we further apply Jacob's scheme [13] for step size adaptation. Let $\alpha_k^{(i)}$ be a single weight of the cost function $L(\alpha^{(i)})$ at the i -th iteration, the corresponding learning rate, $\eta_k^{(i)}$, is updated with the rule

$$\eta_k^{(i+1)} = \begin{cases} \eta_k^{(i)} + \kappa & , \bar{\delta}_k^{(i-1)} \cdot \delta_k^{(i)} > 0 \\ (1 - \gamma)\eta_k^{(i)} & , \bar{\delta}_k^{(i-1)} \cdot \delta_k^{(i)} < 0 \end{cases}, \quad \kappa > 0, \quad 0 < \phi < 1, \quad (4.8)$$

where

$$\delta_k^{(i)} = \frac{\partial L(\alpha^{(i)})}{\partial \alpha_k^{(i)}}, \quad \text{and} \quad \bar{\delta}_k^{(i)} = (1 - \theta)\delta_k^{(i)} + \theta\bar{\delta}_k^{(i-1)}, \quad 0 < \theta < 1.$$

Then the *component-wise* learning rate $\eta^{(i+1)}$ in (4.7) is the diagonal matrix with the (k, k) -th component equal to $\eta_k^{(i+1)}$.

In our computation, we take $\beta = 0.9$, $\gamma = 0.3$, $\theta = 0.7$. The learning rate is uniformly initialized with $\eta_k^{(1)} = \eta_0$, where η_0 is tuned to ensure an efficient and stable convergence. The increase rate of step size κ is set to $\eta_0/10$. The initial guess of parameters is set to $\alpha = \mathbf{0}$ for all test cases. Iterations are stopped when $\|\nabla_{\alpha} L\|_{\infty} < 10^{-3}$ or the maximum iteration of 1000 steps is reached, whichever comes first.

5 Numerical experiments

In this section, we present two numerical experiments to demonstrate that instabilities in plasma can be effectively controlled by the external electric field derived from the moment-based optimization problem (2.9). Additionally, we compare our results with those obtained by controlling instabilities through the full Vlasov-Poisson system-based optimization problem (2.8).

5.1 Suppressing two-stream instability

We consider first the two-stream distribution, which is known to be an unstable equilibrium:

$$\mu(v) = \frac{1}{2\sqrt{2\pi}} \exp\left(-\frac{1}{2}(v - \bar{v})^2\right) + \frac{1}{2\sqrt{2\pi}} \exp\left(-\frac{1}{2}(v + \bar{v})^2\right).$$

Here we take $\bar{v} = 2.4$. The perturbed initial distribution is set to

$$f_0(x, v) = (1 + \varepsilon \cos(0.2x))\mu(v), \quad (x, v) \in [0, 10\pi] \times [-8, 8],$$

where perturbation strength is $\varepsilon = 10^{-3}$. The background ion density is set to $\rho_{ion} = 1$. Periodic boundary conditions are applied at both ends of the spatial interval. The computational domain is discretized by the uniform mesh with $N_x = 100$ and $N_v = 200$ grids in the space and velocity directions.

To suppress the plasma instability, we introduce a time-independent external field taking the form

$$H(x) = \sum_{k=1}^K \alpha_k \sin(\frac{k}{5}x) + \sum_{k=0}^K \beta_k \cos(\frac{k}{5}x), \quad (5.1)$$

where $K = 10$ is chosen to be 10 in the following experiments. We then obtain the optimal $\alpha = \{\alpha_k, \beta_k\}$ by solving the approximate optimization problem (2.9). The approximate electric field $E_N(x, t)$ of the truncated moment system (2.9b) is solved by

$$\begin{cases} E_N = -\partial_x \phi_N, & -\partial_x^2 \phi_N = \rho_N - 1, & \rho_N(x, t) = (2\pi)^{\frac{1}{4}} m_0(x, t) \\ \phi_N(0) = \phi_N(10\pi) = 0. \end{cases}$$

In the test, we truncate (2.9b) at order $N = 30$, and the moment perturbation (2.9a) is minimized at terminal time $T = 30$. The time step of semi-Lagrangian schemes is decided by the following condition

$$\frac{\max_{0 \leq k \leq N} |\lambda_k| \Delta t}{\Delta x} = 3.$$

We denote the resulting external field as H_{mom} .

To verify the effectiveness of H_{mom} in terms of controlling plasma instability as applied to the true physics model (1.3), we substitute H_{mom} into the original Vlasov-Poisson equation and calculate the resulting particle distribution $f(x, v, t; H_{mom})$. Correspondingly, the electric field $E(x, t)$ with respect to the VP system is calculated by

$$\begin{cases} E = -\partial_x \phi, & -\partial_x^2 \phi = \rho - 1, & \rho(x, t) = \int f(x, v, t) dv, \\ \phi(0) = \phi(10\pi) = 0. \end{cases}$$

In our experiments, the Vlasov-Poisson equation is discretized with the semi-Lagrangian scheme following the lines of [7], with the mesh size $N_x = 100$, $N_v = 200$, and the time step $\Delta t = 0.1$.

Figure 5.1 shows the evolution of particle perturbation, $J(t) = \frac{1}{2} \|f(t, \cdot, \cdot) - \mu\|_2^2$, and electric energy, $\mathcal{E}_e(t) = \frac{1}{2} \int E(x, t)^2 dx$, up to $t = 40$. It is seen that when the external field is absent, the initial perturbation is rapidly amplified as time develops, which leads to the deviation of f from μ , as well as the exponential increase in the electric energy. With the help of H_{mom} , such an instability is markedly reduced within the optimization time interval $t \in [0, 30]$. At the terminal time of optimization $T = 30$, H_{mom} suppresses the L^2 -perturbation from $J(30) \approx 0.23$ to 2.71×10^{-5} , and the electric energy from $\mathcal{E}_e(30) \approx 0.75$ to 1.31×10^{-4} . As time evolves further to $t = 40$, H_{mom} can still impose effective control on the instability, reducing $J(40)$ from 0.45 to 6.96×10^{-4} and $\mathcal{E}_e(40)$ from 1.78 to 2.86×10^{-3} . The suppression of perturbation can also be seen from the particle distributions shown in Figure 5.2.

Next, we compare the results generated by H_{mom} optimized against different numbers of moments in the hydrodynamic optimization (2.9). As a reference, we also compute the external field H_{VP} directly optimized against the original kinetic formulation (2.8), that is, the moments are not truncated. The framework of semi-Lagrangian optimization for H_{VP} follows the lines of [7], and the parameter update still follows the momentum gradient descent in Section 4.2. As shown in Figure 5.3, increasing the number of moments included in the optimization leads to a more effective control of the perturbation by the resulting optimized field H_{mom} within the optimization time interval. This is somewhat expected, as the moment system is truncated at a higher order, the objective function (2.9a) provides a tighter upper bound on $\frac{1}{2} \|f(T) - \mu\|_2^2$, and the constraint equations (2.9b) more accurately approximate the true

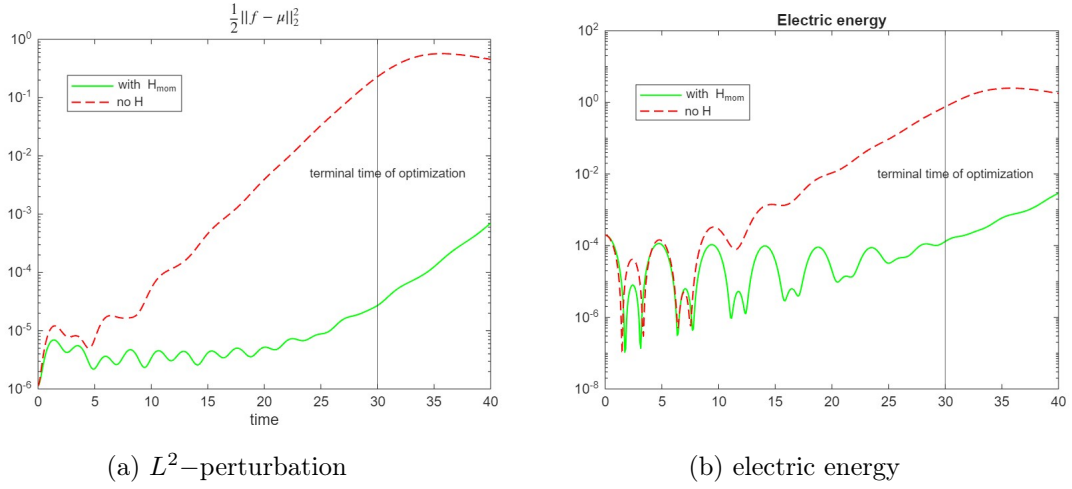


Figure 5.1: Two stream instability. History of perturbation with respect to H_{mom} optimized against $N = 30$ moments. Green lines represent the solutions generated by time-independent H_{mom} . Red lines represent the solutions without external field.

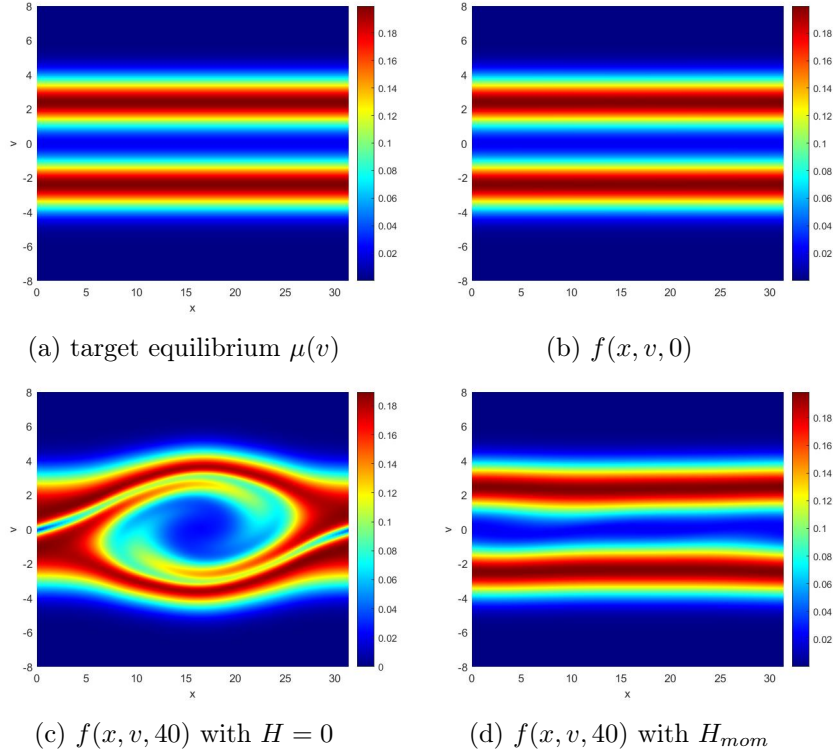


Figure 5.2: Two stream instability. Comparison of particle distributions. H_{mom} is optimized through moment-based optimization (2.9) with $N = 30$.

Vlasov–Poisson dynamics near equilibrium. As a result, the performance of H_{mom} becomes increasingly similar to that of the optimal control field H_{VP} . This can also be seen from the optimized external fields presented in Figure 5.3. However, it is important to note that solving a higher-order moment system incurs increased computational cost, which should be taken into account in practical applications.

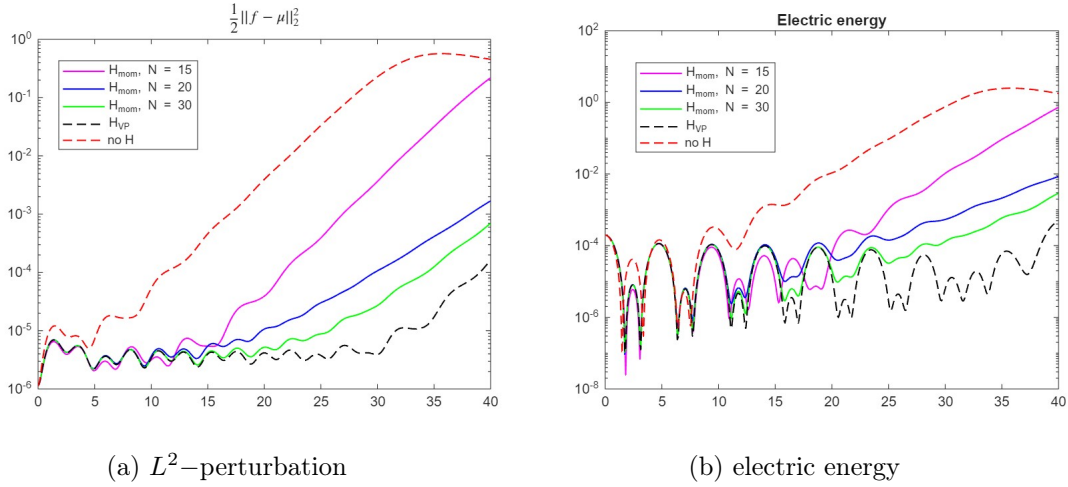


Figure 5.3: Two stream instability. History of perturbation with respect to H_{mom} optimized against different numbers of moments. As the number of moments increases, the result of moment-based optimization approaches that generated by H_{VP} (black dash lines), which indicates the use of full moments.

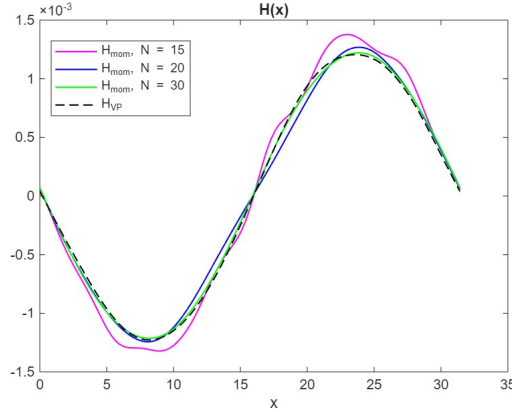


Figure 5.4: Two stream instability. Optimized external fields with respect to different numbers of moments.

5.2 Suppressing Bump-on-tail instability

We next examine the validity of moment based control (2.9) for the bump-on-tail instability. More specially, the equilibrium we consider here takes the form:

$$\mu(v) = \frac{\omega_1}{\sqrt{2\pi}} \exp\left(-\frac{1}{2}v^2\right) + \frac{\omega_2}{\sqrt{2\pi}v_t} \exp\left(-\frac{1}{2v_t}(v-u)^2\right)$$

with $\omega_1 = 0.8$, $\omega_2 = 0.2$, $u = 3.5$, $v_t = 0.5$. The perturbed initial state is set to

$$f_0(x, v) = (1 + \varepsilon \sin(0.2x))\mu(v), \quad (x, v) \in [0, 10\pi] \times [-8, 8].$$

with $\varepsilon = 10^{-3}$. We suppress the instability by introducing external field H_{mom} of the form (5.1) optimized through the problem (2.9) with $T = 25$ and different numbers of moments⁵. $K = 10$ modes are employed

⁵For $N = 15$ and $N = 20$, the iterations do not converge stably with the gradient approximation (4.5), thus their computations are implemented with PyTorch autodifferentiation

to construct H . Again, the computational results displayed in Figures 5.5–5.6 verify that introducing H_{mom} can help suppress the perturbation growth effectively. The improvement in control achieved by using more moments in the optimization is also confirmed. The optimized external fields are presented in Figure 5.7.

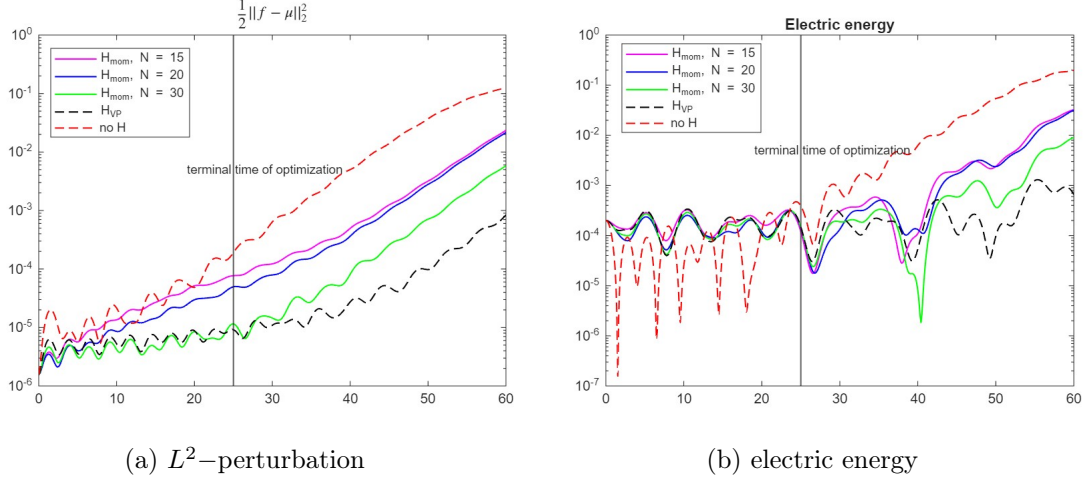


Figure 5.5: Bump-on-tail instability. History of perturbation with respect to H_{mom} optimized against different numbers of moments. Green lines represent the solutions generated by time-independent H_{mom} . Red lines represent the solutions without external field.

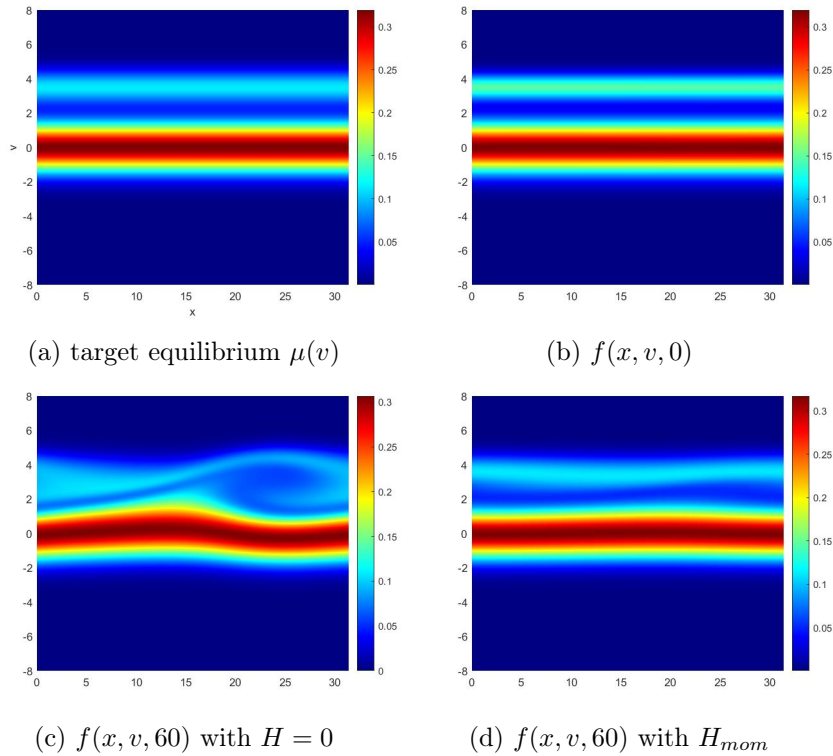


Figure 5.6: Bump-on-tail instability. Comparison of particle distributions. H_{mom} is optimized through moment-based optimization (2.9) with $N = 30$.

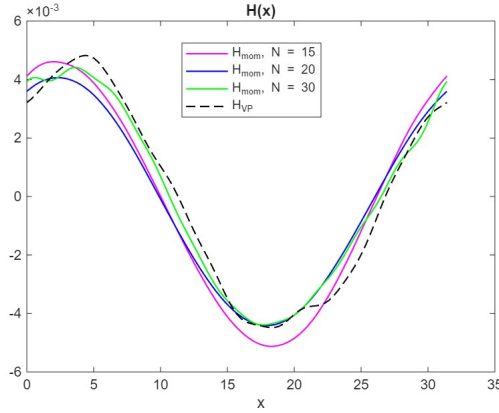


Figure 5.7: Bump-on-tail instability. Optimized external field with respect to different numbers of moments.

Acknowledgment

JL and JC were supported by NSF-CCF:2212318, and JC was additionally supported by an Albert and Dorothy Marden Professorship. LW is supported in part by NSF grant DMS-1846854, DMS-2513336, and the Simons Fellowship. JL and LW would like to thank the fruitful discussion with Professors Michael Herty and Lukas Einkemmer.

References

- [1] G. ALBI, G. DIMARCO, F. FERRARESE, AND L. PARESCHI, *Instantaneous control strategies for magnetically confined fusion plasma*, Journal of Computational Physics, (2025), p. 113804.
- [2] J. BARTSCH, P. KNOPF, S. SCHEURER, AND J. WEBER, *Controlling a Vlasov-Poisson plasma by a Particle-In-Cell method based on a Monte Carlo framework*, arXiv preprint arXiv:2304.02083, (2023).
- [3] M. BESSEMOULIN-CHATARD AND F. FILBET, *On the stability of conservative discontinuous galerkin/hermite spectral methods for the vlasov-poisson system*, Journal of Computational Physics, 451 (2022), p. 110881.
- [4] F. F. CHEN, *Introduction to plasma physics and controlled fusion*, vol. 1, Springer, 2016.
- [5] J. DEGRAVE, F. FELICI, J. BUCHLI, M. NEUNERT, B. TRACEY, F. CARPANESE, T. EWALDS, R. HAFNER, A. ABDOLMALEKI, D. DE LAS CASAS, ET AL., *Magnetic control of tokamak plasmas through deep reinforcement learning*, Nature, 602 (2022), pp. 414–419.
- [6] L. EINKEMMER, Q. LI, C. MOUHOT, AND Y. YUE, *Control of instability in a vlasov-poisson system through an external electric field*, arXiv preprint arXiv:2407.15008, (2024).
- [7] L. EINKEMMER, Q. LI, L. WANG, AND Y. YUNAN, *Suppressing instability in a vlasov-poisson system by an external electric field through constrained optimization*, Journal of Computational Physics, 498 (2024), p. 112662.
- [8] O. GLASS, *On the controllability of the Vlasov-Poisson system*, Journal of Differential Equations, 195 (2003), pp. 332–379.

- [9] O. GLASS AND D. HAN-KWAN, *On the controllability of the Vlasov–Poisson system in the presence of external force fields*, Journal of Differential Equations, 252 (2012), pp. 5453–5491.
- [10] B.-Y. GUO, *Error estimation of hermite spectral method for nonlinear partial differential equations*, Mathematics of Computation, 68 (1999), pp. 1067–1078.
- [11] Y. GUO AND W. A. STRAUSS, *Instability of periodic bgk equilibria*, Communications on Pure and Applied Mathematics, 48 (1995), pp. 861–894.
- [12] J. HUANG, Y. CHENG, A. J. CHRISTLIEB, AND L. F. ROBERTS, *Machine learning moment closure models for the radiative transfer equation i: directly learning a gradient based closure*, Journal of Computational Physics, 453 (2022), p. 110941.
- [13] R. A. JACOBS, *Increased rates of convergence through learning rate adaptation*, Neural networks, 1 (1988), pp. 295–307.
- [14] P. KNOPF, *Optimal control of a Vlasov–Poisson plasma by an external magnetic field*, Calculus of Variations and Partial Differential Equations, 57 (2018), pp. 1–37.
- [15] ———, *Confined steady states of a Vlasov–Poisson plasma in an infinitely long cylinder*, Mathematical Methods in the Applied Sciences, 42 (2019), pp. 6369–6384.
- [16] P. KNOPF AND J. WEBER, *Optimal control of a Vlasov–Poisson plasma by fixed magnetic field coils*, Applied Mathematics & Optimization, 81 (2020), pp. 961–988.
- [17] L. D. LANDAU, *On the vibrations of the electronic plasma*, Uspekhi Fizicheskikh Nauk, 93 (1967), pp. 527–540.
- [18] P.-L. LIONS AND B. PERTHAME, *Propagation of moments and regularity for the 3-dimensional Vlasov–Poisson system*, Inventiones mathematicae, 105 (1991), pp. 415–430.
- [19] J. H. MALMBERG AND C. B. WHARTON, *Collisionless damping of electrostatic plasma waves*, Phys. Rev. Lett., 13 (1964), pp. 184–186.
- [20] C. MOUHOT AND C. VILLANI, *On Landau damping*, Acta Mathematica, 207 (2011), pp. 29–201.
- [21] O. PENROSE, *Electrostatic instabilities of a uniform non-maxwellian plasma*, The Physics of Fluids, 3 (1960), pp. 258–265.
- [22] K. PFAFFELMOSE, *Global classical solutions of the Vlasov–Poisson system in three dimensions for general initial data*, Journal of Differential Equations, 95 (1992), pp. 281–303.
- [23] B. T. POLYAK, *Some methods of speeding up the convergence of iteration methods*, USSR computational mathematics and mathematical physics, 4 (1964), pp. 1–17.
- [24] G. REIN, *Collisionless kinetic equations from astrophysics—the vlasov–poisson system*, in Handbook of differential equations: evolutionary equations, vol. 3, Elsevier, 2007, pp. 383–476.
- [25] J. W. SCHUMER AND J. P. HOLLOWAY, *Vlasov simulations using velocity-scaled hermite representations*, Journal of Computational Physics, 144 (1998), pp. 626–661.
- [26] J. SHEN, T. TANG, AND L.-L. WANG, *Spectral methods: algorithms, analysis and applications*, vol. 41, Springer Science & Business Media, 2011.
- [27] D. SYDORENKO, I. D. KAGANOVICH, P. VENTZEK, AND L. CHEN, *Effect of collisions on the two-stream instability in a finite length plasma*, Physics of Plasmas, 23 (2016).

- [28] T. TANG, *The hermite spectral method for gaussian-type functions*, SIAM journal on scientific computing, 14 (1993), pp. 594–606.
- [29] G. VOGMAN, J. HAMMER, U. SHUMLAK, AND W. FARMER, *Two-fluid and kinetic transport physics of Kelvin–Helmholtz instabilities in nonuniform low-beta plasmas*, Physics of Plasmas, 27 (2020), p. 102109.